

Spectroscopic investigation of volatile compounds produced during thermal and radiofrequency bipolar cautery on porcine liver

To cite this article: J M Rey *et al* 2008 *Meas. Sci. Technol.* **19** 075602

View the [article online](#) for updates and enhancements.

You may also like

- [Rate equations for nitrogen molecules in ultrashort and intense x-ray pulses](#)

Ji-Cai Liu, Nora Berrah, Lorenz S Cederbaum *et al.*

- [Supersymmetry, half-bound states, and grazing incidence reflection](#)

D A Patient and S A R Horsley

- [High-order Ho multipoles in HoB₂C₂ observed with soft resonant x-ray diffraction](#)

A J Princep, A M Mulders, E Schierle *et al.*



The Electrochemical Society
Advancing solid state & electrochemical science & technology

242nd ECS Meeting

Oct 9 – 13, 2022 • Atlanta, GA, US

Abstract submission deadline: **April 8, 2022**

Connect. Engage. Champion. Empower. Accelerate.

MOVE SCIENCE FORWARD



Submit your abstract



Spectroscopic investigation of volatile compounds produced during thermal and radiofrequency bipolar cautery on porcine liver

J M Rey¹, D Schramm¹, D Hahnloser², D Marinov¹ and M W Sigrist¹

¹ Laser Spectroscopy and Sensing Laboratory, Institute for Quantum Electronics, ETH Zurich, Schafmattstr. 16, CH-8093 Zurich, Switzerland

² Department of Visceral and Transplantation Surgery, University Hospital of Zurich, Rämistrasse 100, CH-8091 Zürich, Switzerland

E-mail: sigrist@iqe.phys.ethz.ch

Received 22 November 2007, in final form 28 April 2008

Published 29 May 2008

Online at stacks.iop.org/MST/19/075602

Abstract

The potential risks associated with the emission of by-products emitted by surgical cautery are of concern. Various investigations—mostly based on gas chromatography—have been performed to analyse the so-called surgical smoke but controversies remain in terms of composition and concentrations of compounds present in the smoke and hence the associated risk to human health. This quantitative model study uses for the first time CO₂-laser-based photoacoustic spectroscopy and focuses on the analysis of volatile organic compounds produced during thermal- and radiofrequency bipolar cautery on porcine liver. The latter instrument is employed in actual human surgery. Concentrations in the ppm to sub-ppm range and molar fractions could be determined for carbon dioxide, water vapour, ammonia, ethanol and methanol. Distinct differences particularly in the methanol and ethanol contents were found between the two cautery devices employed.

Keywords: photoacoustic spectroscopy, cautery, volatile compounds

1. Introduction

Cautery surgical devices are based on the conversion of various types of energy into heat. The effect on tissues is thermal and depends on the exposure time and on the amount of energy applied. Tissue reaction to heat depends primarily on the temperature. Cautery begins at temperatures above 60 °C; it is characterized by shrinkage and blanching caused by the denaturation of proteins, particularly collagen [1, 2]. When the tissue temperature reaches 100 °C, the cell water is converted to steam, and the cell wall breaks apart. When the water has evaporated and heat is still applied, the tissue temperature increases rapidly until it reaches 200–300 °C; at this point the tissue burns. The effect of heat on tissue depends also on the exposure time to heat. If heat is applied over a very short

time (less than 1–2 s), the effect is localized because the heat is not conducted to surrounding tissues.

In bipolar electrosurgery an electrical current is passed through the tissue. A generator produces a radiofrequency (RF) current which is transmitted to two electrodes in close proximity; the effect on the tissue is localized, and only a small amount of tissue is affected. When the electrothermal energy is delivered to the vessels, the elastin and collagen of the wall are partially denatured to form a seal. Apart from flowing a current through the tissue, another cautery method consists of using an electrically heated tip to coagulate tissue and to control bleeding. With this method, called thermal cautery, no current flows through the patient. The tip of the cautery instrument is heated by an electric current passing through a resistance wire. The heat transferred by conduction from the

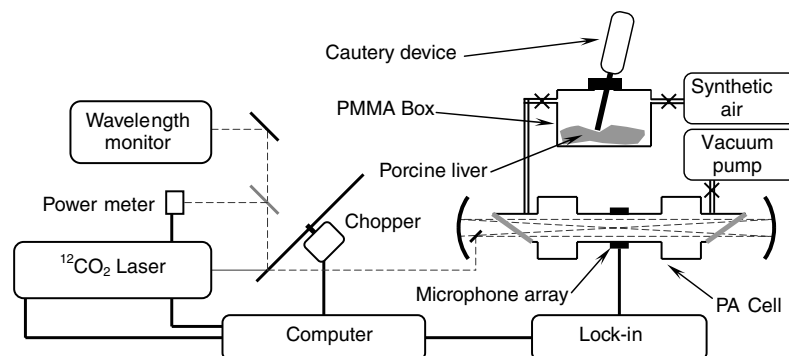


Figure 1. Schematic of the CO₂-laser photoacoustic setup with the PA cell and box in which the smoke is generated by cautery of porcine liver.

tip coagulates the tissue. With thermal cautery radiofrequency interference with other electrical devices is avoided.

Concern about the smoke generated by cautery led to various investigations in order to determine the risks associated with this by-product emission ([3], and references therein). More than 40 different compounds were found in the smoke produced during electrocautery [3], among them carbon dioxide, acrylonitrile, hydrogen cyanide, formaldehyde and benzene being of the most concern. However, previous studies hardly addressed the influence of different surgical instruments and tissue, and controversies remain regarding the emitted compounds and the associated risk to human health. Most of the investigations used gas chromatography (GC) to analyse the smoke compounds previously trapped on a solid adsorbent [4–7].

In this paper, we report on the use of laser photoacoustic (PA) spectroscopy to analyse the smoke generated during thermal and bipolar radiofrequency cautery. PA spectroscopy enables the non-destructive analysis of a gas sample without the need of preconcentration on adsorbent traps. Getting rid of the adsorptive trap reduces the risks of low recovery for the volatile compounds targeted in this study. PA gas sensors are based on the conversion of the absorbed light energy into acoustical waves that can be detected with microphones [8–12]. These sensors allow direct measurement of the small fraction of light absorbed within the PA cell by the gas sample. As a background-free technique, the PA method is highly sensitive. Using a CO₂ laser as the excitation source, PA spectroscopy enables the detection of gases at sub-part-per-billion concentrations of compounds like ammonia, ethylene or methanol [13, 14].

2. Experimental details

Two sealing devices were investigated. The first one, the LigaSure™ (Valleylab, Boulder, CO, USA) vessel sealing system, consists of an RF generator and a dedicated bipolar electrocautery instrument intended for use in laparoscopy. By grasping the tissue with the device and activating the energy source, both physical pressure and electrothermal energy are delivered to the vessels. In operation, the exposed surface of the instrument develops a temperature of approximately

100 °C [15]. The second investigated device consists of an aluminium tip heated with a resistor heater in such a way that the tip temperature is around 100–120 °C when the tip is in contact with the tissue.

Smoke was produced by the application of the two cautery devices (i.e the hot metallic tip and the RF bipolar device) to fresh porcine liver placed in a polymethyl methacrylate (PMMA) box (see figure 1). This box has a volume of 7.2 l and is equipped with connections for gas exchange and for the two sealing devices. In a typical experiment, porcine liver is placed in the PMMA box, which is then sealed and flushed with synthetic air (80% N₂, 20% O₂, purity 5.0, Messer Switzerland). The smoke is generated in the box during a few minutes of cauterization of the porcine liver and then transferred to the PA cell by connecting the box to the previously evacuated PA cell. Synthetic air is then added to the PA cell to reach atmospheric pressure (about 980 mbar).

The PA setup has already been described elsewhere [16]. As figure 1 shows, it consists of a cw sealed-off line-tunable ¹²CO₂ laser (Edinburgh Instruments, model PL-2-L) with a diffraction grating mounted in a Littrow arrangement to set the desired laser transition. An output power of up to 1 W is available depending on the chosen CO₂ laser transition. The CO₂-laser radiation is amplitude-modulated by passing through a chopper (New Focus, model 3501). The laser wavelength is monitored with a spectrum analyser (Optical Engineering, model 16-A) and the actual laser power by a power meter (Coherent Inc., Model 205). The excitation light is coupled into the PA cell. The resonant PA cell is placed in the middle of an Herriott arrangement [17] exhibiting 16 passes. As a result, more laser power is available inside this multipass resonant cell for the generation of the PA signal than in a usual one-pass arrangement. The resonant PA cell consists of five cylinders: the actual resonator (length 120 mm, radius 25 mm), two adjacent buffer volumes with larger diameters (length 60 mm, radius 60 mm) and two cylinders (radius 20 mm) connecting the buffer volumes to the ZnSe-Brewster windows. A radial microphone array with 16 electret microphones (Sennheiser KE 4-211-2) is placed in a plane perpendicular to the optical axis at the centre of the resonator where the first longitudinal resonance of the pressure amplitude reaches its maximum. The signal taken

from the microphone array is monitored by a lock-in amplifier (Stanford Research Systems SR530). The data for the laser power, modulation frequency and the PA signal are recorded on a computer through a GPIB interface. In order to determine the PA cell constant, the system has been calibrated with a certified ethylene gas mixture (AGA Switzerland) diluted to concentrations from 0.5 ppm to 100 ppm using a mass flow controller (Sierra, Serie800). The background signal of the PA system is investigated using the synthetic air used to fill the PMMA box before smoke generation; this residual signal corresponds to an absorption coefficient of $<10^{-6} \text{ cm}^{-1}$.

3. Results and discussion

Thanks to the calibration of the PA system with the ethylene gas mixtures, absolute absorption coefficients of the gas mixture present in the PA cell are obtained at the 55 available CO_2 laser transitions. This permits us to identify and quantify compounds having narrow absorption lines at some specific CO_2 laser transitions. Figure 2(A) presents the photoacoustic spectrum of smoke produced by applying the RF bipolar device to porcine liver. The vertical bars show the absorption coefficient at the various CO_2 laser transitions. Some narrow absorption lines are clearly apparent. Among them the ones at 9P(34) and 9P(14) are assigned to methanol, the ones at 10R(6), 10R(8), 10R(14) and 9R(16) are assigned to ammonia and the ones at 10R(20) and 9R(14) are assigned to water vapour. Using these assignments and the Hitran database [18], the differences between the photoacoustically measured absorption spectra and the simulated Hitran absorption spectra of the four compounds carbon dioxide, methanol, ammonia and water vapour were minimized by fitting with a linear combination of the Hitran spectra for all CO_2 laser transitions. CO_2 absorbs at all CO_2 laser wavelengths without any narrow features. Its concentration is thus approximated by the one needed to null the absorption at any part in the spectrum. Figure 2(B) presents the remaining absorption after removal of the fitted methanol, ammonia, water and carbon dioxide absorptions. This figure points out a broad absorption feature. Even though a CO_2 -laser-based PA system is not designed to investigate broad absorption features, we found good agreement between the remaining absorption and the ethanol spectrum as depicted by the solid line in figure 2(B). Although testing numerous other compounds, only a mixture of gases might match the residual absorption. But by far the best agreement with a single gas was found with ethanol. Other individual molecular spectra such as those of diethylether, butane, pentane, toluene or of many others only yield very unsatisfactory agreement. Hence, this result allowed us to determine the ethanol concentration as given in table 1.

The application of the hot metallic tip to porcine liver yields a rather different smoke spectrum as depicted in figure 3. The same fitting procedure is applied to the measured photoacoustic spectrum. Here also methanol, ammonia and water are identified. The obtained concentrations are also given in table 1. Figure 3(B) presents the absorption spectrum after removal of the fitted methanol, ammonia, water and carbon dioxide absorptions. The remaining spectrum shows

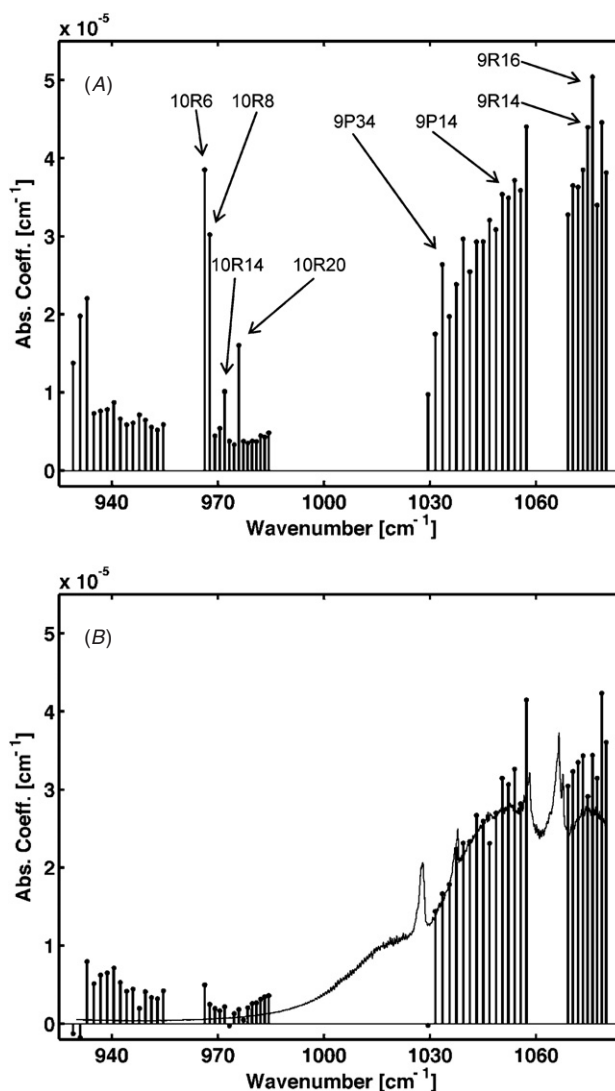


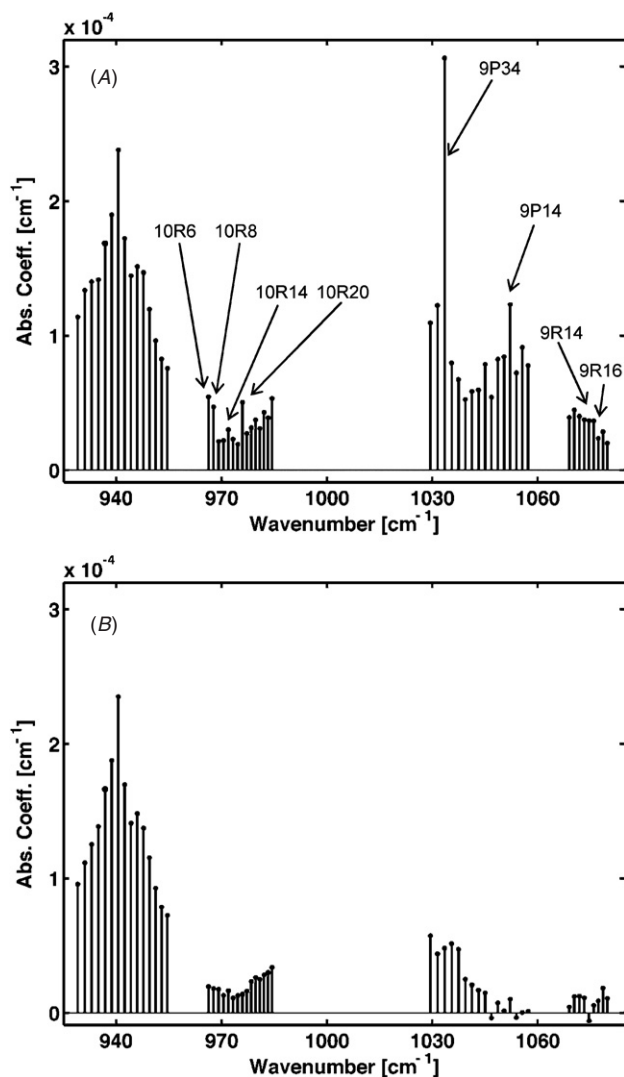
Figure 2. Photoacoustic spectrum (vertical bars) of smoke produced by application of the RF bipolar device to porcine liver. The upper part (A) presents the absorption coefficients derived from the measured photoacoustic spectrum and the lower part (B) shows the remaining absorption after removal of the fitted methanol, ammonia, water vapour and carbon dioxide concentrations (see the text). The full line in part (B) shows the estimated ethanol absorption.

some broad absorption features that cannot be assigned to ethanol unlike the smoke spectrum obtained with the RF bipolar device. This absorption feature could not be assigned due to the limited tuning range of the CO_2 laser system. Further investigations using another laser source having a broader tuning range would help identifying the compounds responsible for the remaining absorptions.

Although the PA setup allows determination of the absolute absorption coefficients of a sample, the molar fractions of the identified compounds are of greater interest since they are much less influenced by the variability in the smoke sampling procedure. These molar fractions are also given in table 1. The results imply that the bipolar RF device generates more ethanol than methanol and that the metallic tip

Table 1. Measured concentrations and their corresponding molar fraction for the identified compounds in smoke produced by using the RF bipolar device and the hot metallic tip on porcine liver.

| Identified compounds | RF bipolar device | | Hot metallic tip | |
|----------------------|------------------------------|----------------------|------------------------------|----------------------|
| | Measured concentration (ppm) | Molar fraction | Measured concentration (ppm) | Molar fraction |
| Methanol | 0.2 ± 0.1 | 0.4×10^{-3} | 14 ± 0.2 | 14×10^{-3} |
| Ethanol | 5 ± 0.5 | 9.8×10^{-3} | 0 ± 0.5 | 0.0×10^{-3} |
| Ammonia | 0.7 ± 0.5 | 1.4×10^{-3} | 0.7 ± 0.1 | 0.7×10^{-3} |
| Water vapour | 2.3 ± 0.5 | 4.5×10^{-3} | 4.8 ± 0.5 | 4.7×10^{-3} |
| Carbon dioxide | 500 ± 300 | 0.98 | 1000 ± 500 | 0.98 |

**Figure 3.** Photoacoustic spectrum (vertical bars) of smoke produced by application of the hot metallic tip to porcine liver. The upper part (A) presents the absorption coefficients derived from the measured photoacoustic spectrum and the lower part (B) shows the remaining absorption after removal of the fitted methanol, ammonia, water vapour and carbon dioxide concentrations (see the text).

does the opposite (i.e. generates more methanol than ethanol). The water vapour and carbon dioxide molar fractions are similar for the two cauterization processes but the bipolar RF device

generates proportionally twice as much ammonia. The CO₂-laser PA system with detection limits in the ppb range [13] used here is a sensitive tool for detecting ethylene, which was not observed here. This permits us to conclude that the concentration of ethylene was below 100 ppb in the generated smoke.

The volatile compounds present in the smoke are a combination of low-molecular weight products from the degradation of amino acids and lipid oxidation as well as further reaction products from these degradation compounds. Ammonia is produced by hydrolysis of dicarboxylic amino acids in proteins and its production increases with temperature [19]. The higher ammonia fraction observed with the RF device is thus an indication of the slightly higher tissue temperature obtained with this device. This can be explained by the more efficient energy transfer to the tissue obtained with the RF electromagnetic field, which does not rely solely on thermal diffusion. Alcohols in the tissue smoke are believed to originate from reduction of aldehydes obtained from oxidation of lipids and amino acids [20]. Depending on the reductive conditions different alcohols are produced. The fact that the ratio between emitted methanol and ethanol strongly depends on the cauterization technique indicates that both methods generate different chemical conditions in the cauterization zone.

4. Conclusion

Using a CO₂-laser-based photoacoustic spectrometer, surgical smokes emitted during purely thermal and bipolar RF cauterization on porcine liver were investigated. This spectroscopic technique allowed us to obtain the molar fraction of five volatile compounds: methanol, ethanol, ammonia, water and carbon dioxide. Both cauterization methods generate comparable water and carbon dioxide molar fractions but lead to significantly different ammonia, methanol and ethanol molar fractions. Differences in the latter molar fractions are presumably due to the different temperature and chemical (i.e. redox) properties present in the cauterization zone. It should be emphasized that gas adsorption at the cell walls (kept at room temperature) may influence the results of individual measurements. However, since this study compares two different kinds of cauterization processes and the derived concentrations are in the ppm and not ppb range, adsorption effects can be neglected. Furthermore, some experiments have been performed twice without major differences between the derived gas concentrations. This is also confirmed by previous experiments [21].

References

- [1] McKenzie A L 1986 A three-zone model of soft-tissue damage by a CO₂ laser *Phys. Med. Biol.* **31** 967–83
- [2] Walsh J T Jr, Flotte T J, Anderson R R and Deutsch T F 1988 Pulsed CO₂ laser tissue ablation: effect of tissue type and pulse duration on thermal damage *Lasers Surg. Med.* **8** 108–18
- [3] Barrett W L and Garber S M 2003 Surgical smoke—a review of the literature. Is this just a lot of hot air? *Surg. Endosc.* **17** 979–87
- [4] Hensman C, Baty D, Willis R G and Cuschieri A 1988 Chemical composition of smoke produced by high-frequency electrosurgery in a closed gaseous environment *Surg. Endosc.* **12** 1017–19
- [5] Spleiss M and Weber L 1996 Medium and low volatile organic compounds generated by laser tissue interaction *Proc. SPIE* **2923** 168–77
- [6] Waesche W and Albrecht H A 1996 Investigation of the distribution of aerosols and VOC in plume produced during laser treatment under OR conditions *Proc. SPIE* **2624** 270–75
- [7] Albrecht H, Hagemann R, Waesche W, Wagner G and Mueller G 1994 Volatile organic components in laser and electrosurgery plume *Proc. SPIE* **2077** 310–17
- [8] Sigrist M W 1994 Air monitoring by laser photoacoustic spectroscopy *Air Monitoring by Spectroscopic Techniques* ed M W Sigrist (*Chemical Analysis Series* vol 127) (New York: Wiley) pp 163–238
- [9] Harren F J M, Cotti G, Oomens J and te L Hekkert L 2000 Photoacoustic spectroscopy in trace gas monitoring *Encyclopedia of Analytical Chemistry* vol 3 ed R A Meyers (Chichester: Wiley) pp 2203–26
- [10] Miklòs A and Hess P 2001 Application of acoustic resonators in photoacoustic trace gas analysis and metrology *Rev. Sci. Instrum.* **72** 1937–55
- [11] Patterson C S, McMillan L C, Longbottom C, Gibson G M, Padgett M J and Skeldon K D 2007 Portable optical spectroscopy for accurate analysis of ethane in exhaled breath *Meas. Sci. Technol.* **18** 1459–64
- [12] Webber M E, MacDonald T, Pushkarsky M B, Patel C K N, Zhao Y, Marcillac N and Mitloehner F M 2005 Agricultural ammonia sensor using diode lasers and photoacoustic spectroscopy *Meas. Sci. Technol.* **16** 1547–53
- [13] Naegele M and Sigrist M W 2000 Mobile laser spectrometer with novel resonant multipass photoacoustic cell for trace-gas sensing *Appl. Phys. B* **70** 895–901
- [14] Pushkarsky M B, Webber M E and Patel C K N 2003 Ultra-sensitive ambient ammonia detection using CO₂-laser-based photoacoustic spectroscopy *Appl. Phys. B* **77** 381–5
- [15] Campbell P A, Cresswell A B, Frank T G and Cuschieri A 2003 Real-time thermography during energized vessel sealing and dissection *Surg. Endosc.* **17** 1640–5
- [16] Rey J M, Marinov D, Vogler D E and Sigrist M W 2005 Investigation and optimisation of a multipass resonant photoacoustic cell at high absorption levels *Appl. Phys. B* **80** 261–6
- [17] McManus J B, Keabian P L and Zahniser M S 1995 Astigmatic mirror multipass absorption cells for long-path-length spectroscopy *Appl. Opt.* **34** 3336–48
- [18] Rothman L S et al 2005 The HITRAN 2004 molecular spectroscopic database *J. Quantum Spectrosc. Radiat. Transfer* **96** 139–204
- [19] Schultz H S, Day E A and Libbey L M 1967 Flavor of red meats *The Chemistry and Physiology of Flavors* (Westport, CT: Avi Publishing Company) pp 241–4
- [20] Barbieri G, Bolzoni L, Parolari G, Virgili R, Buttini R, Careri M and Mangia A 1992 Flavor compounds of dry-cured ham *J. Agric. Food Chem.* **40** 2389–94
- [21] Hollmann R, Hort C E, Kammer E, Naegele M, Sigrist M W and Meuli-Simmen C 2004 Smoke in the operating theatre—an unregarded source of danger *Plast. Reconstr. Surg.* **114** 458–63